

# Convex quantization preserves logconcavity

Pol del Aguila Pla, *Member, IEEE*, Aleix Boquet-Pujadas, Joakim Jaldén, *Senior Member, IEEE*

**Abstract**—Much like convexity is key to variational optimization, a logconcave distribution is key to amenable statistical inference. Quantization is often disregarded when writing likelihood models: ignoring the limitations of physical detectors. This begs the questions: would including quantization preclude logconcavity, and, are the true data likelihoods logconcave? We show that the same simple assumption that leads to logconcave continuous data likelihoods also leads to logconcave quantized data likelihoods, provided that convex quantization regions are used.

**Index Terms**—Variational inverse problems, Bayesian statistics, Logconcavity, Quantization

## I. INTRODUCTION

Inference from signals in the digital domain is of central importance in digital signal processing. However, the discrete nature of measurement devices is often disregarded or misrepresented in building data likelihood models. When quantization is deemed fine enough, the established procedure is to ignore it or to model it as additive noise [1], [2]. At the opposite end, the few works that investigate coarse quantization do so under strong simplifying assumptions [3]–[5], suggesting that optimal estimation might be intractable.

Explicitly considering quantization has been increasingly popular [3]–[7] due to the advent of 1-bit compressed sensing techniques and the promise of incorporating low-cost high-speed analog-to-digital converters (ADC) into wireless communications’ pipelines.

Quantization is also influential in the privacy-enhancement literature [8], [9]. Besides simple noise addition mechanisms, coarse quantization or “aggregation” is one of the simplest techniques to induce differential privacy and  $k$ -anonymity on a database. However, privacy protection and data utility are conflicting objectives. To better understand this tradeoff in aggregation-based techniques, it is fundamental to characterize the properties of the data likelihood after quantization.

Variational inverse problems with convex data terms, which can be interpreted as maximum-a-posteriori (MAP) estimators for logconcave likelihood models, also typically ignore data quantization to build their cost functions. However, examples where quantization plays a crucial role abound in applications (see Figure 1): think of honeycomb electrode detectors [10] in high energy physics, of the sinogram-domain quantization induced by the geometry of positron emission tomography

(PET) scanners, of the pixelized detectors in computed tomography [11], or of CCD and CMOS photodetectors in biological microscopy [12]. Furthermore, we expect that image reconstruction algorithms that use the full Bayesian paradigm will benefit even further from treating quantization explicitly, because they use the entire posterior distribution to make inferences. This is in contrast to using only the mean or the mode, which are much more easily conserved between quantized and continuous data.

Admittedly, however, incorporating quantization into likelihood models challenges theoretical guarantees that are otherwise automatic under most common noise models (e.g., Gaussian or exponential) due to likelihood logconcavity. Examples include tractable maximum likelihood (ML) and MAP estimates, connected and convex credible and confidence sets, and large sample normal approximations that lead to tractable hypothesis testing [13]. In order to recover these properties, most works that address quantization either resort to simplifying assumptions such as Gaussian data and 1-bit quantization [3]–[5], or optimistically assume logconcavity [6], [7], [9].

In this article, we prove that the logconcavity of a quantized likelihood follows from the same assumption made on its continuous counterpart—logconcavity of the noise distribution. The result holds for convex quantizers, which do not only include all the examples mentioned so far, but an overwhelming majority of applications. In practice, this means that likelihood-based methods automatically enjoy convergence guarantees when accounting for a plethora of detector models, and, therefore, that more accurate models can be readily adopted. We expect that the convenience of this result will encourage researchers to more often include quantized models and thus better capture the nature of measurement devices. In a similar vein, another aim of this manuscript is to publicize and exploit a series of techniques that are part of the folklore of the statistics’ literature, but are yet to make the transition to the signal processing community [14]. For example, while not entirely new to our community [15]–[17], Prékopa’s results [18] on logconcavity are key to this work and have not previously been harnessed in their full generality.

To the best of our knowledge, our analysis is the most general treatment of likelihood logconcavity for quantized data yet. Our study also considers the scale parameter, which had only been previously considered for a concrete application in [4]. Furthermore, we appear to be the first to do the analysis for a generic vector quantizer  $Q$  more general than simple combinations of independent ADCs.

## II. LOGCONCAVITY FOR CONTINUOUS DATA

Our central claim is that for both continuous and quantized data, likelihood logconcavity will follow from the logconcavity

Pol del Aguila Pla is with the CIBM Center for Biomedical Imaging, in Switzerland.

Pol del Aguila Pla and Aleix Boquet-Pujadas are with the Biomedical Imaging Group at the École polytechnique fédérale de Lausanne, in Lausanne, Switzerland.

Joakim Jaldén is with the Division of Information Science and Engineering at the School of Electrical Engineering and Computer Science at the KTH Royal Institute of Technology, in Stockholm, Sweden.

of the noise pdf. In particular, consider a data vector  $\mathbf{y} \in \mathbb{R}^n$  modeled as

$$\mathbf{y} = \Psi^{-1}(\mathbf{S}\mathbf{x} + \mathbf{w}), \quad (1)$$

where  $\Psi \in \mathcal{M}_n^+(\mathbb{R})$  is a real positive-definite matrix,  $\mathbf{S} \in \mathcal{M}_{n,m}(\mathbb{R})$  is a  $n \times m$  matrix,  $\mathbf{x} \in \mathbb{R}^m$ , and  $\mathbf{w} \in \mathbb{R}^n$  is a random noise vector  $\mathbf{w} \sim f_{\mathbf{w}}(\mathbf{w})$  drawn from a logconcave pdf, i.e.,

$$f_{\mathbf{w}}(\mathbf{w}_\alpha) \geq f_{\mathbf{w}}(\mathbf{w}_1)^\alpha f_{\mathbf{w}}(\mathbf{w}_0)^{(1-\alpha)}. \quad (2)$$

Here,  $\mathbf{w}_\alpha := \alpha \mathbf{w}_1 + (1-\alpha)\mathbf{w}_0$  with  $\alpha \in [0,1]$  is a convex combination between  $\mathbf{w}_0$  and  $\mathbf{w}_1$ . Throughout the paper, we will resort to this notation for convex combinations for simplicity of exposition. The case  $\Psi = \mathbf{I}$  in (1) corresponds to a usual linear model formulation, where  $\mathbf{S}$  is the observation matrix. In statistics,  $\mathbf{x}$  and  $\Psi$  in (1) are known as the location and scale parameters of the distribution family defined by (1). For example, if the noise comes from a standard multivariate normal distribution  $\mathbf{w} \sim \mathcal{N}(\mathbf{0}, \mathbf{I})$ , we have that  $\mathbf{y} \sim \mathcal{N}(\Psi^{-1}\mathbf{S}\mathbf{x}, \Psi^{-2})$ . For each data vector  $\mathbf{y} \in \mathbb{R}^n$ , the likelihood is a function of the location and scale parameters  $\mathcal{L}(\cdot, \cdot; \mathbf{y}) : \mathbb{R}^m \times \mathcal{M}_n^+(\mathbb{R}) \rightarrow \mathbb{R}_+$  such that

$$\mathcal{L}(\mathbf{x}, \Psi; \mathbf{y}) := f_{\mathbf{y}; \mathbf{x}, \Psi}(\mathbf{y}) = f_{\mathbf{w}}(\Psi\mathbf{y} - \mathbf{S}\mathbf{x}), \quad (3)$$

where we used (1) to write  $\mathcal{L}(\mathbf{x}, \Psi; \mathbf{y})$  in terms of  $f_{\mathbf{w}}(\cdot)$ .

The following result sets the stage for our study.

**Theorem 1** (Logconcave Noise Generates Logconcave Likelihoods). *Consider a sample  $\mathbf{y} \in \mathbb{R}^n$  drawn from model (1) and assume that the pdf of the noise,  $f_{\mathbf{w}}(\cdot)$ , is logconcave. Then,  $\mathcal{L}(\mathbf{x}, \Psi; \mathbf{y})$  is jointly logconcave in  $\mathbf{x}$  and  $\Psi$ .*

*Proof.* Using (3), we obtain

$$\begin{aligned} \mathcal{L}(\mathbf{x}_\alpha, \Psi_\alpha; \mathbf{y}) &= f_{\mathbf{w}}(\Psi_\alpha \mathbf{y} - \mathbf{S}\mathbf{x}_\alpha) \\ &\geq f_{\mathbf{w}}([\Psi_1 \mathbf{y} - \mathbf{S}\mathbf{x}_1])^\alpha f_{\mathbf{w}}([\Psi_0 \mathbf{y} - \mathbf{S}\mathbf{x}_0])^{1-\alpha}, \end{aligned}$$

which is the desired result. Here, we used (2) with

$$\mathbf{w}_i = \Psi_i \mathbf{y} - \mathbf{S}\mathbf{x}_i \text{ for } i \in \{0, 1\}.$$

□

*Remark 2* (Parametrization of Location-Scale Statistical Models). Although the location-scale parametrization in (1) is less familiar than, say, the mean and covariance matrices in multivariate Gaussian models, this choice is intentional and essentially related to the study of logconcavity. In fact, in order to show that joint estimators of  $\boldsymbol{\mu}$  and  $\boldsymbol{\Sigma}$  in a  $\mathcal{N}(\boldsymbol{\mu}, \boldsymbol{\Sigma})$  model are tractable, one needs to first reparametrize the problem in terms of  $\mathbf{x}$  and  $\Psi$ .

### III. LOGCONCAVITY FOR QUANTIZED DATA

It turns out that a statement similar to Theorem 1 can be made for quantized observations  $z \in \mathcal{Z}$  modeled as

$$z = Q(\mathbf{y}) = Q(\Psi^{-1}(\mathbf{S}\mathbf{x} + \mathbf{w})). \quad (4)$$

Here, we take the most general view of quantization: we define a quantizer as a mapping  $Q : \mathbb{R}^n \rightarrow \mathcal{Z}$ , where  $\mathcal{Z}$  is a countable set. These quantizers need not necessarily treat each dimension

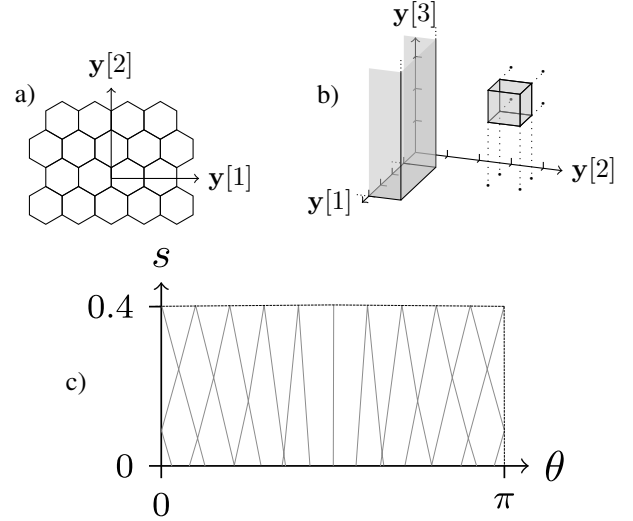


Fig. 1. a) Convex regions laid down according to a honeycomb pattern such as done for hexagonal electrode detectors. b) Two quantization regions of a convex quantizer formed by independent ADCs. c) Example quantization regions of a PET scanner in sinogram domain.

of  $\mathbf{y}$  independently. The results we present hereafter apply to the subclass of quantizers with convex quantization regions, i.e., quantizers  $Q$  such that  $Q^{-1}(z)$  is a convex set  $\forall z \in \mathcal{Z}$ ; we will refer to these as convex quantizers. Among others introduced beforehand, these include quantizers composed of independent (monotonic) ADCs for each dimension (see Figure 1b). Indeed, in that case, for any  $z \in \mathcal{Z}$ , there are  $\{a_j\}, \{b_j\} \subset \mathbb{R}$  such that  $Q^{-1}(z) = \prod_{j=1}^n [a_j, b_j]$ , which is trivially convex. Our main result below parallels Theorem 1 for quantized data obtained from convex quantizers.

**Theorem 3** (Logconcave Noise and Convex Quantizers Generate Logconcave Likelihoods). *Consider a sample  $z \in \mathcal{Z}$  drawn from model (4). Assume that  $Q$  is a convex quantizer and that the pdf  $f_{\mathbf{w}}(\cdot)$  of the noise is logconcave. Then,*

- for a given scale parameter  $\Psi_0 \in \mathcal{M}_n^+(\mathbb{R})$ , the likelihood  $\mathcal{L}(\mathbf{x}, \Psi_0; z)$  is logconcave with respect to  $\mathbf{x}$ ,
- for scale parameters of the form  $\Psi = \psi \mathbf{I}$  with  $\psi > 0$ , the likelihood  $\mathcal{L}(\mathbf{x}, \psi \mathbf{I}; z)$  is jointly logconcave with respect to  $\mathbf{x}$  and  $\psi$ ,
- for diagonal positive-definite scale parameters  $\Psi = \Lambda$ , the likelihood  $\mathcal{L}(\mathbf{x}, \Lambda; z)$  is jointly logconcave with respect to  $\mathbf{x}$  and  $\Lambda$  if  $Q$  is composed of independent ADCs for each dimension.

### IV. MATHEMATICAL STUDY OF LOGCONCAVITY UNDER QUANTIZATION

The rest of this work is dedicated to proving Theorem 3. We first construct the likelihood of the location and scale parameters for a given  $z \in \mathcal{Z}$ . Observing  $z$  under model (4) implies, by definition, that  $\mathbf{y} \in Q^{-1}(z)$ . This, in turn, implies that the random noise  $\mathbf{w}$  is within a specific region. For specific values of  $\mathbf{x}$  and  $\Psi$ , and for each  $z \in \mathcal{Z}$ , we define

$$\mathcal{W}_z(\mathbf{x}, \Psi) := \{\mathbf{w} \in \mathbb{R}^n : \mathbf{y} \in Q^{-1}(z)\} \quad (5)$$

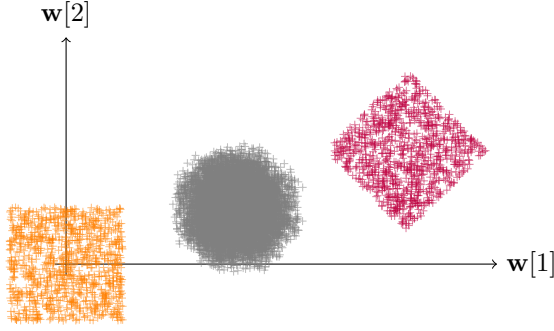


Fig. 2. Example of the Minkowski sum of two sets scaled by  $\alpha = 1/2$  (in the center). Each set is represented here by random elements within it.

as a shorthand for this region. We then write the likelihood as

$$\mathcal{L}(\mathbf{x}, \Psi; z) = P_{\mathbf{w}}[\mathcal{W}_z(\mathbf{x}, \Psi)], \quad (6)$$

where  $P_{\mathbf{w}}$  denotes the probability law in  $\mathbb{R}^n$  given by the pdf  $f_{\mathbf{w}}(\cdot)$ .

Our strategy to prove Theorem 3 combines this compact expression of the quantized-data likelihood with a key result by Prékopa, which we include here for completeness.

**Theorem 4** (Prékopa's Theorem [18, p. 2, Th. 2]). *Let  $\mathbf{w}$  be a continuous random variable in  $\mathbb{R}^n$  with logconcave pdf  $f_{\mathbf{w}}(\mathbf{w})$ , in the sense of (2). Let  $P_{\mathbf{w}} : 2^{\mathbb{R}^n} \rightarrow [0, 1]$  be the probability measure induced by  $\mathbf{w}$  on  $\mathbb{R}^n$ . Then, for any two convex sets  $\mathcal{A}_0, \mathcal{A}_1 \subseteq \mathbb{R}^n$  we have that*

$$P_{\mathbf{w}}[\mathcal{A}_\alpha] \geq P_{\mathbf{w}}[\mathcal{A}_1]^\alpha P_{\mathbf{w}}[\mathcal{A}_0]^{(1-\alpha)}, \quad (7)$$

where  $\mathcal{A}_\alpha$  is the Minkowski sum  $\alpha\mathcal{A}_1 + (1-\alpha)\mathcal{A}_0$ .

Here, the weighted Minkowski sum  $\mathcal{A}_\alpha$  (illustrated in Figure 2) is the set of all possible combinations  $\mathbf{w}_\alpha = \alpha\mathbf{w}_1 + (1-\alpha)\mathbf{w}_0$  in which  $\mathbf{w}_1 \in \mathcal{A}_1$ ,  $\mathbf{w}_0 \in \mathcal{A}_0$ , for a given value  $\alpha \in [0, 1]$ . The Minkowski sum preserves convexity: if  $\mathcal{A}_1$  and  $\mathcal{A}_2$  are convex, then  $\mathcal{A}_\alpha$  is also convex.

To prove Theorem 3, we identify the sets  $\mathcal{W}_z(\mathbf{x}_\alpha, \Psi_\alpha)$  in (5) with the sets  $\mathcal{A}_\alpha$  in Theorem 4. Then, (7) becomes the desired logconcavity statement. The technical conditions of Theorem 3, therefore, only ensure that the convex combination of location and scale parameters leads to the same set  $\mathcal{W}_z(\mathbf{x}_\alpha, \Psi_\alpha)$  as the Minkowski sum of the corresponding scaled sets  $\mathcal{W}_z(\mathbf{x}_i, \Psi_i)$  for  $i \in \{0, 1\}$ . We start by verifying convexity in the extreme cases  $\alpha \in \{0, 1\}$ .

**Lemma 5** (Convex Quantizers Lead to Convex Noise Regions). *For any  $z \in \mathcal{Z}$ ,  $\mathbf{x} \in \mathbb{R}^m$ , and  $\Psi \in \mathcal{M}_n^+(\mathbb{R})$ ,  $\mathcal{W}_z(\mathbf{x}, \Psi)$  is convex if and only if  $Q^{-1}(z)$  is convex.*

*Proof.* Let  $\mathbf{w}_0, \mathbf{w}_1 \in \mathcal{W}_z(\mathbf{x}, \Psi)$ . Then,  $\mathbf{w}_i = \Psi\mathbf{y}_i - \mathbf{S}\mathbf{x}$  for  $\mathbf{y}_i \in Q^{-1}(z)$  with  $i \in \{0, 1\}$ . Because  $Q^{-1}(z)$  is convex,  $\mathbf{y}_\alpha \in Q^{-1}(z)$ , and therefore,  $\mathbf{w}_\alpha = \Psi\mathbf{y}_\alpha - \mathbf{S}\mathbf{x}_\alpha \in \mathcal{W}_z(\mathbf{x}, \Psi)$ . In conclusion, if  $Q^{-1}(z)$  is convex,  $\mathcal{W}_z(\mathbf{x}, \Psi)$  is convex.

For the converse, simply consider that  $\mathcal{W}_z(\mathbf{0}, \mathbf{I}) = Q^{-1}(z)$ .  $\square$

This allows us to set

$$\mathcal{A}_i = \mathcal{W}_z(\mathbf{x}_i, \Psi_i) \text{ for } i \in \{0, 1\}, \quad (8)$$

while fulfilling the conditions of Theorem 4. For the intermediate values  $\alpha \in (0, 1)$ , we identify conditions under which  $\mathcal{W}_z(\mathbf{x}_\alpha, \Psi_\alpha)$  is the Minkowski sum of  $\alpha\mathcal{A}_1$  and  $(1-\alpha)\mathcal{A}_0$ . We start by identifying that one of the inclusions is always fulfilled.

**Lemma 6.** *Consider  $\mathcal{A}_0$  and  $\mathcal{A}_1$  as defined in (8). Then  $\mathcal{W}_z(\mathbf{x}_\alpha, \Psi_\alpha) \subseteq \mathcal{A}_\alpha$ .*

*Proof.* Let  $\mathbf{w} \in \mathcal{W}_z(\mathbf{x}_\alpha, \Psi_\alpha)$ . Then, there is  $\mathbf{y} \in Q^{-1}(z)$  such that

$$\begin{aligned} \mathbf{w} &= \Psi_\alpha \mathbf{y} - \mathbf{S}\mathbf{x}_\alpha \\ &= \alpha\mathbf{w}_1 + (1-\alpha)\mathbf{w}_0, \end{aligned}$$

with  $\mathbf{w}_i = \Psi_i \mathbf{y} - \mathbf{S}\mathbf{x}_i$  for  $i \in \{0, 1\}$ . By definition,  $\mathbf{w}_i \in \mathcal{A}_i$ .  $\square$

The opposite inclusion is harder to obtain. To show it, we will need intermediate results on the geometry of sets generated by matrices that sum to  $\mathbf{I}$ , which we include in the Appendix. In fact, the inclusion is generally not true when one considers generic scale parameters (see Lemma 9 in the Appendix). However, by restricting them as in Theorem 3, we obtain the following.

**Lemma 7.** *Consider  $\mathcal{A}_0$  and  $\mathcal{A}_1$  as defined in (8). If for  $i \in \{0, 1\}$ ,*

- $\Psi_1 = \Psi_0$ , or,
- $\Psi_i = \psi_i \mathbf{I}$  with  $\psi_i > 0$ , or,
- $\Psi_i = \Lambda_i$  with  $\Lambda_i \in \mathcal{D}_n^+$  and  $Q^{-1}(z) = \prod_{j=1}^n [a_j, b_j]$  with  $a_j, b_j \in \mathbb{R}$ ,

then  $\mathcal{A}_\alpha \subseteq \mathcal{W}_z(\mathbf{x}_\alpha, \Psi_\alpha)$ .

*Proof.* Let  $\alpha_0 = 1 - \alpha$  and  $\alpha_1 = \alpha$  and consider the matrices

$$\mathbf{C}_i = (\alpha_0 \Psi_0 + \alpha_1 \Psi_1)^{-1} \alpha_i \Psi_i$$

for  $i \in \{0, 1\}$ . Consider also that  $\mathbf{C}_0 + \mathbf{C}_1 = \mathbf{I}$ .

Let  $\mathbf{w} \in \mathcal{A}_\alpha$ . Then, there are  $\mathbf{w}_i \in \mathcal{A}_i$  for  $i \in \{0, 1\}$  such that  $\mathbf{w} = \alpha_0 \mathbf{w}_0 + \alpha_1 \mathbf{w}_1$ . Furthermore, by (8) we have that  $\mathbf{w}_i = \Psi_i \mathbf{y}_i - \mathbf{S}\mathbf{x}_i$  for  $i \in \{0, 1\}$ , where  $\mathbf{y}_i \in Q^{-1}(z)$ . Therefore,

$$\begin{aligned} \mathbf{w} &= \sum_{i=0}^1 (\alpha_i \Psi_i \mathbf{y}_i - \mathbf{S}\alpha_i \mathbf{x}_i) \\ &= (\alpha_0 \Psi_0 + \alpha_1 \Psi_1) (\mathbf{C}_0 \mathbf{y}_0 + \mathbf{C}_1 \mathbf{y}_1) - \mathbf{S}(\alpha_0 \mathbf{x}_0 + \alpha_1 \mathbf{x}_1). \end{aligned}$$

By definition, then,  $\mathbf{w} \in \mathcal{W}_z(\mathbf{x}_\alpha, \Psi_\alpha)$  if and only if  $\mathbf{y} = \mathbf{C}_0 \mathbf{y}_0 + \mathbf{C}_1 \mathbf{y}_1 \in Q^{-1}(z)$ .

If condition a) is fulfilled, then  $\mathbf{C}_i = \alpha_i \mathbf{I}$  and  $\mathbf{y} = \mathbf{y}_\alpha$ . Because  $Q^{-1}(z)$  is convex,  $\mathbf{y} \in Q^{-1}(z)$ . If condition b) is fulfilled, then  $\mathbf{C}_i = \tilde{\alpha}_i \mathbf{I}$  with  $\tilde{\alpha}_i = \alpha_i \psi_i / (\alpha_0 \psi_0 + \alpha_1 \psi_1)$ , and  $\mathbf{y}$  is a convex combination of  $\mathbf{y}_0$  and  $\mathbf{y}_1$ , i.e.,  $\mathbf{y} = \mathbf{y}_{\tilde{\alpha}}$ . Because  $Q^{-1}(z)$  is convex,  $\mathbf{y} \in Q^{-1}(z)$ . If condition c) is fulfilled, then the  $\mathbf{C}_i$ s are diagonal matrices with elements between 0 and 1, i.e.,  $\mathbf{C}_i \in \mathcal{D}_n([0, 1])$ . By Lemma 8 in the Appendix, we then have  $\mathbf{y} \in \prod_{j=1}^n [y_1[j], y_2[j]]$ . Because  $Q^{-1}(z) = \prod_{j=1}^n [a_j, b_j]$ , and  $a_j \leq y_1[j], y_2[j] \leq b_j$ ,  $\mathbf{y} \in Q^{-1}(z)$ . Therefore, if either a), b) or c) are given,  $\mathbf{w} \in \mathcal{W}_z(\mathbf{x}_\alpha, \Psi_\alpha)$ .  $\square$

We can now combine Lemmas 5–7 with Theorem 4 to show Theorem 3.

*Proof of Theorem 3.* Consider  $\mathcal{A}_0$  and  $\mathcal{A}_1$  as defined in (8). By Lemma 5, they are convex sets. By Lemmas 6 and 7, if a), b) or c) are fulfilled, we have that  $\mathcal{A}_\alpha = \mathcal{W}_z(\mathbf{x}_\alpha, \Psi_\alpha)$ . Then, Theorem 4 and (6) yield

$$\begin{aligned} \mathcal{L}(\mathbf{x}_\alpha, \Psi_\alpha; z) &= P_{\mathbf{w}}[\mathcal{A}_\alpha] \\ &\geq P_{\mathbf{w}}[\mathcal{A}_1]^\alpha P_{\mathbf{w}}[\mathcal{A}_0]^{(1-\alpha)} \\ &= \mathcal{L}(\mathbf{x}_1, \Psi_1; z)^\alpha \mathcal{L}(\mathbf{x}_0, \Psi_0; z)^{1-\alpha}. \end{aligned}$$

□

## V. ACKNOWLEDGMENTS

We acknowledge access to the facilities and expertise of the CIBM Center for Biomedical Imaging, a Swiss research center of excellence founded and supported by Lausanne University Hospital (CHUV), University of Lausanne (UNIL), École polytechnique fédérale de Lausanne (EPFL), University of Geneva (UNIGE), and Geneva University Hospitals (HUG).

This work was partially supported by the SRA ICT TNG project Privacy-preserved Internet Traffic Analytics (PITA).

## APPENDIX MATRIX COMBINATIONS

In Lemma 7, we use that sets of the form  $\prod_{j=1}^n [a_j, b_j]$  with  $a_j, b_j \in \mathbb{R}$  are closed with respect to the generalization of convex combinations to diagonal matrices. In Fig. 3a, we include an illustration of a practical case in 2D. Here, we provide the proof. To our knowledge, this has not been reported before.

**Lemma 8** (Diagonal Matrices Whose Sum is the Identity Generate Squares). *Let  $\mathcal{D}_n([0, 1])$  be the set of square  $n$ -dimensional diagonal matrices with elements in  $[0, 1]$ , and let  $\mathbf{y}_0, \mathbf{y}_1 \in \mathbb{R}^n$ . Then,*

$$\begin{aligned} \mathcal{H} &:= \{\mathbf{C}\mathbf{y}_0 + (\mathbf{I} - \mathbf{C})\mathbf{y}_1 : \mathbf{C} \in \mathcal{D}_n[0, 1]\} \\ &= \prod_{j=1}^n [y_0[j], y_1[j]] =: \mathcal{H}_{\blacksquare}. \end{aligned}$$

*Proof.* For  $\mathcal{H}_{\blacksquare} \subseteq \mathcal{H}$ , let  $\mathbf{y} \in \mathcal{H}_{\blacksquare}$ . If  $\alpha_j = (\mathbf{y}[j] - \mathbf{y}_1[j]) / (\mathbf{y}_0[j] - \mathbf{y}_1[j])$ , then  $\alpha_j \in [0, 1]$ . If  $\mathbf{C} \in \mathcal{D}_n([0, 1])$  is the diagonal matrix such that  $\mathbf{C}[j, j] = \alpha_j$ , then  $\mathbf{C}\mathbf{y}_0 + (\mathbf{I} - \mathbf{C})\mathbf{y}_1 = \mathbf{y}$ . Thus,  $\mathbf{y} \in \mathcal{H}$ .

For  $\mathcal{H} \subseteq \mathcal{H}_{\blacksquare}$ , let  $\mathbf{y} \in \mathcal{H}$ . Then, we have that  $\alpha_j = \mathbf{C}[j, j] \in [0, 1]$ , and  $\mathbf{y}[j] = \alpha_j \mathbf{y}_1[j] + (1 - \alpha_j) \mathbf{y}_0[j]$ , and thus,  $\mathbf{y}[j] \in [y_0[j], y_1[j]]$ . Therefore,  $\mathbf{y} \in \mathcal{H}_{\blacksquare}$ . □

On the one hand, the result in Lemma 8 allows for the most general result in terms of the scale parameter  $\Psi$  we have obtained (Theorem 3.c). On the other hand, the corresponding result in the following lemma suggests that the strategy behind our proof might not generalize well to arbitrary scale parameters. We include it here for completeness, and because, to our knowledge, it has not been reported before.

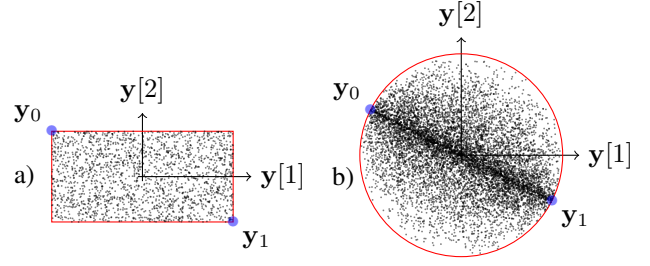


Fig. 3. In black, points obtained by combinations with matrices whose sum is the identity matrix, i.e.,  $\mathbf{C}\mathbf{y}_1 + (\mathbf{I} - \mathbf{C})\mathbf{y}_0$ , where  $\mathbf{C}$  were, in a), random diagonal matrices from  $\mathcal{D}_n([0, 1])$ , and, in b), random positive semidefinite matrices from  $\mathcal{M}_n^+(\mathbb{R})$  with  $\rho(\mathbf{C}) \leq 1$ . In blue,  $\mathbf{y}_0$  and  $\mathbf{y}_1$ .

**Lemma 9** (Positive Semidefinite Matrices that Sum to the Identity Generate Balls<sup>1</sup>). *Let  $\mathcal{M}_n^{\oplus}(\mathbb{R})$  be the set of real symmetric positive semidefinite matrices with spectral radius less or equal than 1, i.e.,  $\rho(\mathbf{C}) \leq 1$ , and  $\mathbf{y}_0, \mathbf{y}_1 \in \mathbb{R}^n$ . Then*

$$\begin{aligned} \mathcal{S} &:= \{\mathbf{C}\mathbf{y}_0 + (\mathbf{I} - \mathbf{C})\mathbf{y}_1 : \mathbf{C} \in \mathcal{M}_n^{\oplus}(\mathbb{R})\} \\ &= \mathcal{B}\left(\frac{\mathbf{y}_0 + \mathbf{y}_1}{2}, \frac{1}{2} \|\mathbf{y}_1 - \mathbf{y}_0\|_2\right) =: \mathcal{S}_{\bullet}, \end{aligned}$$

where  $\mathcal{B}(\mathbf{y}_c, r)$  is the closed  $\ell_2$  ball centered at  $\mathbf{y}_c \in \mathbb{R}^n$  with radius  $r \geq 0$ .

*Proof.* For  $\mathcal{S}_{\bullet} \subseteq \mathcal{S}$ , let  $\mathbf{y} \in \mathcal{S}$ . Then, there is a  $\mathbf{C} \in \mathcal{M}_n^{\oplus}(\mathbb{R})$  such that  $\mathbf{y} = \mathbf{C}\mathbf{y}_0 + (\mathbf{I} - \mathbf{C})\mathbf{y}_1$ . If  $\mathbf{y}_c = (\mathbf{y}_0 + \mathbf{y}_1)/2$ , then

$$\begin{aligned} \|\mathbf{y} - \mathbf{y}_c\|_2 &= \left\| \left(\mathbf{C} - \frac{\mathbf{I}}{2}\right) (\mathbf{y}_0 - \mathbf{y}_1) \right\|_2 \\ &\leq \left\| \mathbf{C} - \frac{\mathbf{I}}{2} \right\|_{2 \rightarrow 2} \|\mathbf{y}_0 - \mathbf{y}_1\|_2 \\ &\leq \frac{1}{2} \|\mathbf{y}_1 - \mathbf{y}_0\|_2. \end{aligned}$$

Therefore,  $\mathbf{y} \in \mathcal{S}_{\bullet}$ . Here, we have used that the operator norm of a matrix with respect to the  $\ell_2$  norm coincides with the spectral radius  $\rho(\cdot)$  for Hermitian matrices.

For  $\mathcal{S}_{\bullet} \subseteq \mathcal{S}$ , let  $\mathbf{y} \in \mathcal{S}_{\bullet}$  and  $\mathbf{y}_c = (\mathbf{y}_0 + \mathbf{y}_1)/2$ . Then, consider  $\tilde{\mathbf{y}} = \mathbf{y} - \mathbf{y}_1$  and  $\tilde{\mathbf{y}}_0 = \mathbf{y}_0 - \mathbf{y}_1$ . Because  $\mathbf{y} \in \mathcal{S}_{\bullet}$ , we have that  $\|\tilde{\mathbf{y}} - \tilde{\mathbf{y}}_0/2\|_2^2 = \|\mathbf{y} - \mathbf{y}_c\|_2^2 \leq (\|\mathbf{y}_1 - \mathbf{y}_0\|_2/2)^2 = (\|\tilde{\mathbf{y}}_0\|_2/2)^2$ . Expanding the squares, we obtain  $0 \leq \|\tilde{\mathbf{y}}\|_2^2 \leq \tilde{\mathbf{y}}_0^T \tilde{\mathbf{y}}$ . If we consider then the matrix  $\mathbf{C} = \tilde{\mathbf{y}} \tilde{\mathbf{y}}^T / \tilde{\mathbf{y}}^T \tilde{\mathbf{y}}_0$ , we see that it is a rank 1 matrix with a single non-zero eigenvalue  $\lambda = \text{tr}(\mathbf{C}) = \|\tilde{\mathbf{y}}\|_2^2 / \tilde{\mathbf{y}}^T \tilde{\mathbf{y}}_0 \in [0, 1]$ , i.e.,  $\mathbf{C} \in \mathcal{M}_n^{\oplus}(\mathbb{R})$ . Furthermore,  $\mathbf{C}(\mathbf{y}_0 - \mathbf{y}_1) = \mathbf{C}\tilde{\mathbf{y}}_0 = \tilde{\mathbf{y}} = \mathbf{y} - \mathbf{y}_1$ , i.e.,  $\mathbf{y} = \mathbf{C}\mathbf{y}_0 + (\mathbf{I} - \mathbf{C})\mathbf{y}_1$ . Therefore,  $\mathbf{y} \in \mathcal{S}$ . □

*Remark 10.* To apply our proof technique for Lemma 7 to arbitrary scale parameters  $\Psi \in \mathcal{M}_n^+(\mathbb{R})$ , we would need to restrict the quantization regions so that  $\mathbf{y}_0, \mathbf{y}_1 \in \mathcal{Q}^{-1}(z)$  implies  $\mathcal{S}_{\bullet} \subset \mathcal{Q}^{-1}(z)$ . Our intuitive understanding is that only trivial quantizers would fulfill this property.

However, because Theorem 4 is sufficient but not necessary, Lemma 9 does not preclude likelihood logconcavity results for that case.

<sup>1</sup>See [www.geogebra.org/m/hdxtmz3b](http://www.geogebra.org/m/hdxtmz3b) and [www.geogebra.org/m/tskjev2m](http://www.geogebra.org/m/tskjev2m) for 2D and 3D dynamic examples of this lemma based on the SVD of any positive semidefinite matrix.

## REFERENCES

- [1] B. Widrow and I. Kollár, *Quantization noise: Roundoff error in digital computation, signal processing, control, and communications*. Cambridge University Press, 2008.
- [2] A. Azizzadeh, R. Mohammadkhani, S. V. A.-D. Makki, and E. Björnson, "BER performance analysis of coarsely quantized uplink massive MIMO," *Signal Processing*, 2019.
- [3] S. Li, X. Li, X. Wang, and J. Liu, "Decentralized sequential composite hypothesis test based on one-bit communication," *IEEE Transactions on Information Theory*, no. 99, 2017.
- [4] J. Ren, T. Zhang, J. Li, and P. Stoica, "Sinusoidal parameter estimation from signed measurements via majorization-minimization based RELAX," *IEEE Transactions on Signal Processing*, 2019.
- [5] S. Khobahi, N. Naimipour, M. Soltanalian, and Y. C. Eldar, "Deep signal recovery with one-bit quantization," in *2019 IEEE International Conference on Acoustics, Speech and Signal Processing (ICASSP)*, 2019.
- [6] C. K. Wen, C. J. Wang, S. Jin, K. K. Wong, and P. Ting, "Bayes-optimal joint channel-and-data estimation for massive MIMO with low-precision ADCs," *IEEE Transactions on Signal Processing*, vol. 64, no. 10, pp. 2541–2556, May 2016.
- [7] M. S. Stein, S. Bar, J. A. Nossek, and J. Tabrikian, "Performance analysis for channel estimation with 1-bit ADC and unknown quantization threshold," *IEEE Transactions on Signal Processing*, vol. 66, no. 10, pp. 2557–2571, May 2018.
- [8] C. C. Aggarwal and P. S. Yu, "A general survey of privacy-preserving data mining models and algorithms," in *Privacy-Preserving Data Mining*. Springer, 2008, pp. 11–52.
- [9] P. Gao, R. Wang, M. Wang, and J. H. Chow, "Low-rank matrix recovery from noisy, quantized, and erroneous measurements," *IEEE Transactions on Signal Processing*, vol. 66, no. 11, pp. 2918–2932, Jun. 2018.
- [10] Y. Zhang, C. Liao, M. Liu, S. Lu, and Z. Li, "Optimization of 3D shell electrode detectors—A type of honeycomb shell electrode detector," *AIP Advances*, vol. 8, no. 12, p. 125309, 2018.
- [11] M. Danielsson, M. Persson, and M. Sjölin, "Photon-counting x-ray detectors for CT," *Physics in Medicine & Biology*, vol. 66, no. 3, p. 03TR01, Jan 2021.
- [12] G. Köklü, J. Ghaye, R. Beuchat, G. De Micheli, Y. Leblebici, and S. Carrara, "Quantitative comparison of commercial ccd and custom-designed cmos camera for biological applications," in *2012 IEEE International Symposium on Circuits and Systems (ISCAS)*, 2012, pp. 2063–2066.
- [13] J. W. Pratt, "Concavity of the log likelihood," *Journal of the American Statistical Association*, vol. 76, no. 373, pp. 103–106, 1981.
- [14] J. Burridge, "Some unimodality properties of likelihoods derived from grouped data," *Biometrika*, vol. 69, no. 1, pp. 145–151, 1982.
- [15] S. Boyd and L. Vandenberghe, *Convex optimization*. Cambridge University Press, 2004.
- [16] A. Conti, D. Panchenko, S. Sidenko, and V. Tralli, "Log-concavity property of the error probability with application to local bounds for wireless communications," *IEEE Transactions on Information Theory*, vol. 55, no. 6, pp. 2766–2775, Jun. 2009.
- [17] E. J. Msechu and G. B. Giannakis, "Sensor-centric data reduction for estimation with WSNs via censoring and quantization," *IEEE Transactions on Signal Processing*, vol. 60, no. 1, pp. 400–414, Jan. 2012.
- [18] A. Prékopa, "Logarithmic concave measures and functions," *Acta Scientiarum Mathematicarum*, vol. 34, no. 1, pp. 334–343, 1973.